Supplemental Figure legends:

Fig. S1 **Reactions of ZPI mutants with factor XIa**-Progress curves for reactions of 110 nM wild-type and mutant ZPIs as indicated with 0.25 nM factor XIa. Solid lines are fits to an exponential function.

Fig. S2 **Native PAGE of purified ZPI variants-** Lanes 1-8, Wild-type and mutant ZPIs as indicated; lane 9, PZ. The D74/D293 double mutant band is barely detectable because of its altered charge and reduced ability to enter the gel.

Fig. S3 **7.5% SDS-PAGE of purified recombinant PZ-PC chimeras**- Lane 1, 83, 62, 47, and 32 kDa standards; lane 2, wild-type PZ; lane 3, PZ/PC (Gla); lane 4, PZ/PC (EGF1); lane 5, PZ/PC (EGF2); lane 6, PZ/PC (Gla-EGF2). The PZ/PC (EGF1) and PZ/PC (Gla-EGF2) forms migrate with a lower apparent molecular weight due to the absence of an N-linked carbohydrate (at N59) in the EGF1 domain of PZ.

Fig S4 **Native PAGE analysis of cZPI binding to PZ**- Lane 1, native ZPI, lane 2, cZPI, lane 3, cZPI+PZ, lane 4, native ZPI+PZ, lane 5, PZ; ~3 μM ZPI, cZPI and PZ were analyzed. The low intensity of the cZPI band results from poor staining with Coomassie dye.

Fig. S5 **Simulations of PZ catalysis of the ZPI-factor Xa reaction at physiologic levels of ZPI and PZ-** Simulations assumed the standard serpin reaction scheme with PZ-ZPI complex as the inhibitor, a partitioning ratio of 1:2 for reaction of the PZ-ZPI-FXa acyl-intermediate along inhibitor and substrate pathways and kinetic constants measured previously for the PZ-dependent reaction in the presence of 25 μM lipid and 5 mM Ca^{2+} under approximate physiologic conditions.[11] For ZPI-PZ interactions, a diffusion-limited k_{on} of 10^7 $M^{-1}s^{-1}$ was assumed and k_{off} values were calculated assuming measured K_Ds of 1.2 and 6.8 nM for PZ interactions with native and cZPI. Progress curves for the indicated species were simulated using Kintech software with normal plasma concentrations of 53 nM ZPI and 47 nM PZ reacting with 3.33 nM factor Xa. The

simulations show the disappearance of ZPI-PZ binary complex and factor Xa and the concomitant appearance of the initial products, the PZ-cZPI-FXa and PZ-cZPI complexes, followed by decreases in these PZ complexes and concomitant increases in cZPI-FXa, cZPI and ZPI-PZ binary complexes due to 52% PZ dissociation from the product cZPI complexes (10 nM total) and rebinding to free ZPI. Dashed lines show the final ZPI-PZ complex levels when PZ binds ZPI and cZPI with equal affinity (no catalysis) or when PZ completely loses affinity for cZPI (full catalysis).

Fig. S6 **X-ray structures of cZPI in the helix A region-** A, Overlay of cZPI (I2) structure (green) with cZPI (P41) structure (yellow) in the helix A/helix D region. The structures differ only in the helix D position, suggesting flexibility of the helix. B, Overlay of native ZPI (cyan) and cZPI (I2) (green) structures in ribbon on the left highlights the bent helix A of native ZPI but straight helix in cZPI. The top right shows that the bending of helix A (orange) in native ZPI is induced by interactions of W46 (yellow spacefill) of helix A with neighboring leucines (green spacefill). The bottom right shows that helix A is straight in cZPI because the stressed to relaxed conformational transition disrupts the W46 interactions.

Fig. S7 **Comparison of the X-ray structures of free mouse ZPI and the human ZPI-PZ complex-** A, X-ray structure of mouse ZPI in ribbon colored as in Fig. 7A. B, Overlay of mouse ZPI (green) with the human ZPI-PZ complex (cyan) shows that free and complexed ZPIs are similar except for the RCL and helix A and that helix G structure is retained.

Fig. S8 **Shifting of the alpha-carbons of the key PZ binding residues of ZPI following the stressed to relaxed conformational transition-** Distances between M71 and D293 consistently change by around 0.7Å between native ZPI (C) and either of the two cZPI structures (A & B) whereas other distances change by less than 0.3 Å between native and cleaved structures.

Table S1: *Crystallographic data collection and refinement statistics*

	cZPI (I2)	cZPI (P41)	Native mouse ZPI
Data collection			
Space group	I2	P41	P3212
Unit-cell parameters (a,b,c, Å ; α,β,γ, °)	78.85, 106.66, 81.16 90.00, 112.58, 90.00	100.70, 100.70, 78.97 90, 90, 90	83.53, 83.53, 181.26, 90, 90, 120
Solvent content	63.33%	71.14%	69.70%
Molecules per ASU	1	1	1
Resolution range	44.39-2.09 (2.20-2.09)	100.26-2.65 (2.79-2.65)	37.37-2.5 (2.64-2.50)
Unique reflection	31054(4654)	22072(2733)	25077 (3494)
Average redundancy	2.8(2.7)	3.0 (2.8)	5.3 (5.5)
Completeness (%)	84.3 (87.0)	95.8 (82.2)	98 (94.4)
Average I/sigma	6.9(1.8)	9.9 (1.5)	4.9 (1.6)
R_{merge}	0.075(0.471)	0.068 (0.720)	0.27 (1.063)
R_{meas}	0.091(0.577)	0.083 (0.880)	0.298 (1.171)
Refinement statistics			
Number of residues	413	400	383
Number of refined atoms	3126	3148	3044
R value	0.210	0.215	0.23
R_{free} value	0.249	0.258	0.27
RMS bond length (Å)	0.008	0.007	0.008
RMS bond angles(°)	1.441	1.001	1.052
Ramachandran plot (favoured/outliers, %)	97.88% / 0%	96.55% / 0%	98.10%/0%
Mean B-factor	33.5	19.8	57.62
MolProbity Score*	1.53(97%)	1.77(99%)	1.48(99%)
PDB code	4AFX	4AJU	4AJT

100^{th} percentile is the best among structures of comparable resolution; 0^{th} percentile is the worst.

Table S2: *Kinetic constants and stoichiometries of inhibition for ZPI-factor XIa reactions in the absence of cofactors*- Second order rate constants (k_{ass}) for reactions of wild-type and mutant ZPIs with factor XIa were determined from the slope of linear plots of k_{obs} on ZPI concentration in the range 25-125 nM. Stoichiometries of inhibition (SI) for factor XIa were measured from the endpoints of reactions containing ~100 nM factor XIa active sites and ZPI concentrations ranging from 200-800 nM. The product of k_{ass} and SI represents the corrected association rate constant for reaction through the inhibitory pathway.

ZPI	ZPI-FXIa reactions		
	$k_{ass,app}$ ($M^{-1}s^{-1}$)	SI (mol I/ mol E)	$k_{ass,app}$ x SI ($M^{-1}s^{-1}$)
Wild-type	$1.4\pm0.1 \times 10^5$	8.0±0.3	$1.1\pm0.1 \times 10^6$
M71A	$1.4\pm0.1 \times 10^5$	8.5±0.2	$1.2\pm0.1 \times 10^6$
D74A	$1.3\pm0.1 \times 10^5$	9.2±0.3	$1.2\pm0.1 \times 10^6$
D238A	$7.4\pm0.5 \times 10^4$	14.7±0.2	$1.1\pm0.1 \times 10^6$
K239A	$1.2\pm0.1 \times 10^5$	9.4±0.2	$1.1\pm0.1 \times 10^6$
Y240A	$1.2\pm0.1 \times 10^5$	10.3±0.4	$1.2\pm0.1 \times 10^6$
D293A	$1.0\pm0.1 \times 10^5$	10.6±0.3	$1.1\pm0.1 \times 10^6$
D74A/D293A	$1.4\pm0.1 \times 10^5$	12.2±0.1	$1.7\pm0.1 \times 10^6$

Table S3: *Analysis of mutated ZPI residues in the binding interface with PZ using the PDBePISA server (Protein* Interfaces*, Surfaces and Assemblies)* (http://www.ebi.ac.uk/msd-srv/prot_int/cgi-bin/piserver). ZPI residues in ZPI-PZ complex structure, 3F1S, making **H**ydrogen/**D**isulphide bond, **S**alt bridge or **C**ovalent links; **ASA,** Accessible Surface Area, Å²; **BSA,** Buried Surface Area, Å²; **Δ^iG,** Solvation energy effect, kcal/mol; ||||, Buried area percentage, one bar per 10%. Note that Met71, Lys239, Tyr240 and Asp293 sidechains are buried to similar extents and Lys239 and Asp293 make similar hydrogen bonding and salt bridge interactions, yet these residues make vastly different contributions to binding. Similarly, the relative contributions of Asp74 and Asp238 to binding are not correlated with their buried surface area.

ZPI residue	HSDC	ASA	BSA	Δ^iG
Met71	H	172.15	156.23 |||||||||	2.58
Asp74	HS	100.26	45.67 |||||	-0.47
Asp238	S	64.81	41.98 |||||||	0.11
Lys239	HS	145.66	124.44 ||||||||	-0.22
Tyr240		207.28	180.88 ||||||||	1.42
Asp293	HS	106.44	96.13 |||||||||	-0.62

Fig. S1

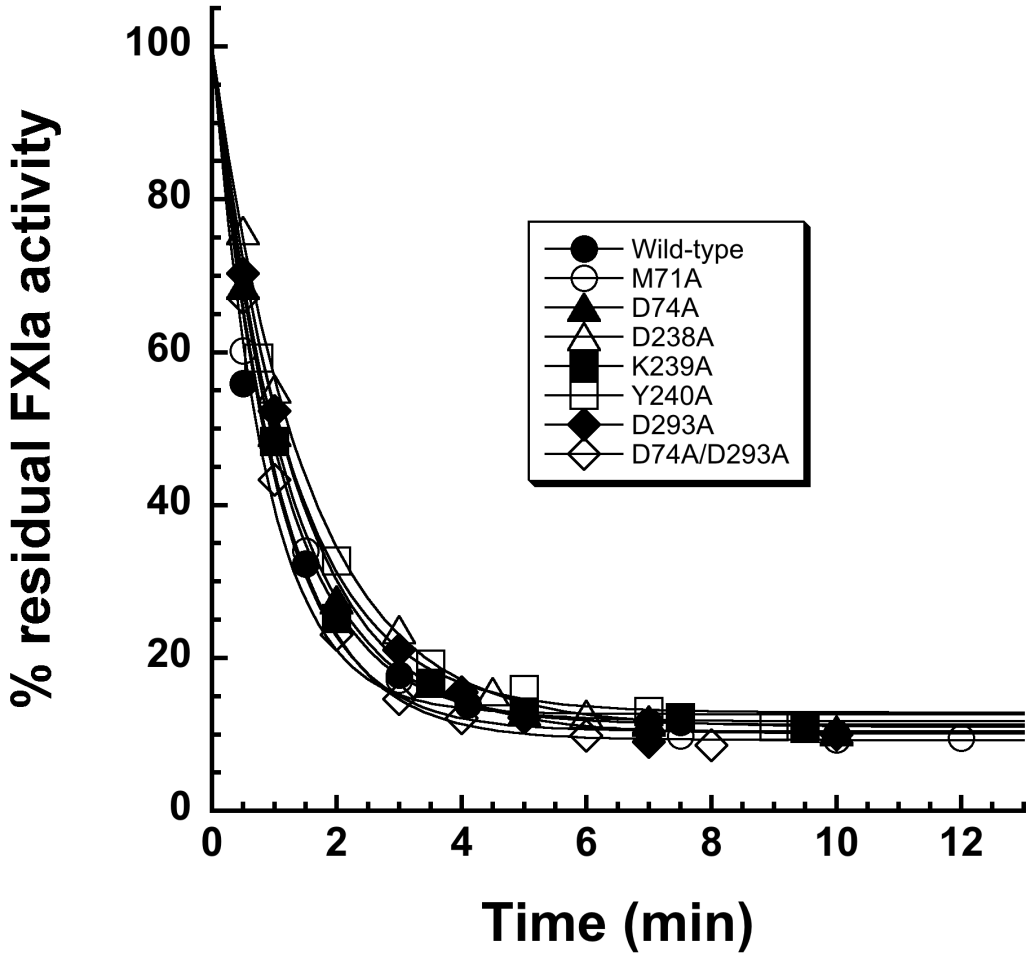
% residual FXIa activity
100
80
60
40
20
0
0
2
4
6
8
10
12
Time (min)
Wild-type
M71A
D74A
D238A
K239A
Y240A
D293A
D74A/D293A

Fig. S2

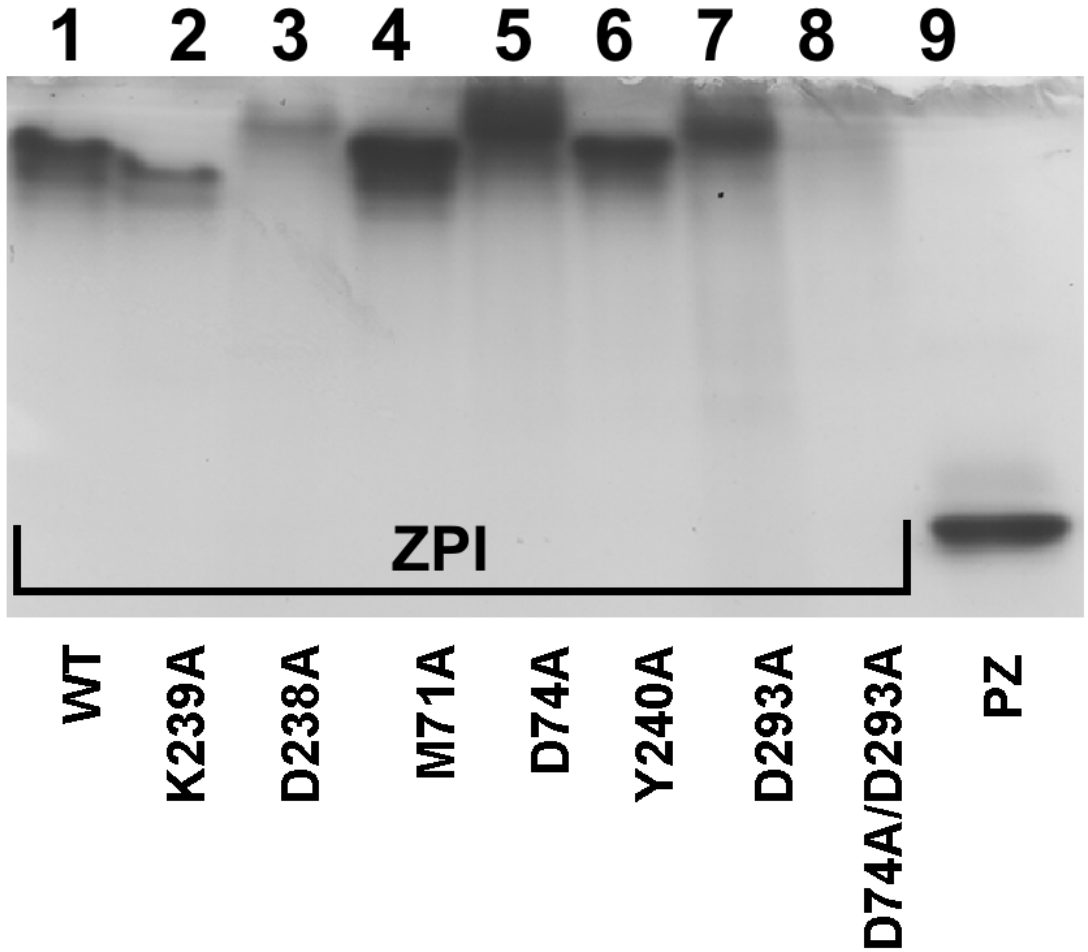
1
2
3
4
5
6
7
8
9
ZPI
WT
K239A
D238A
M71A
D74A
Y240A
D293A
D74A/D293A
PZ

Fig. S3

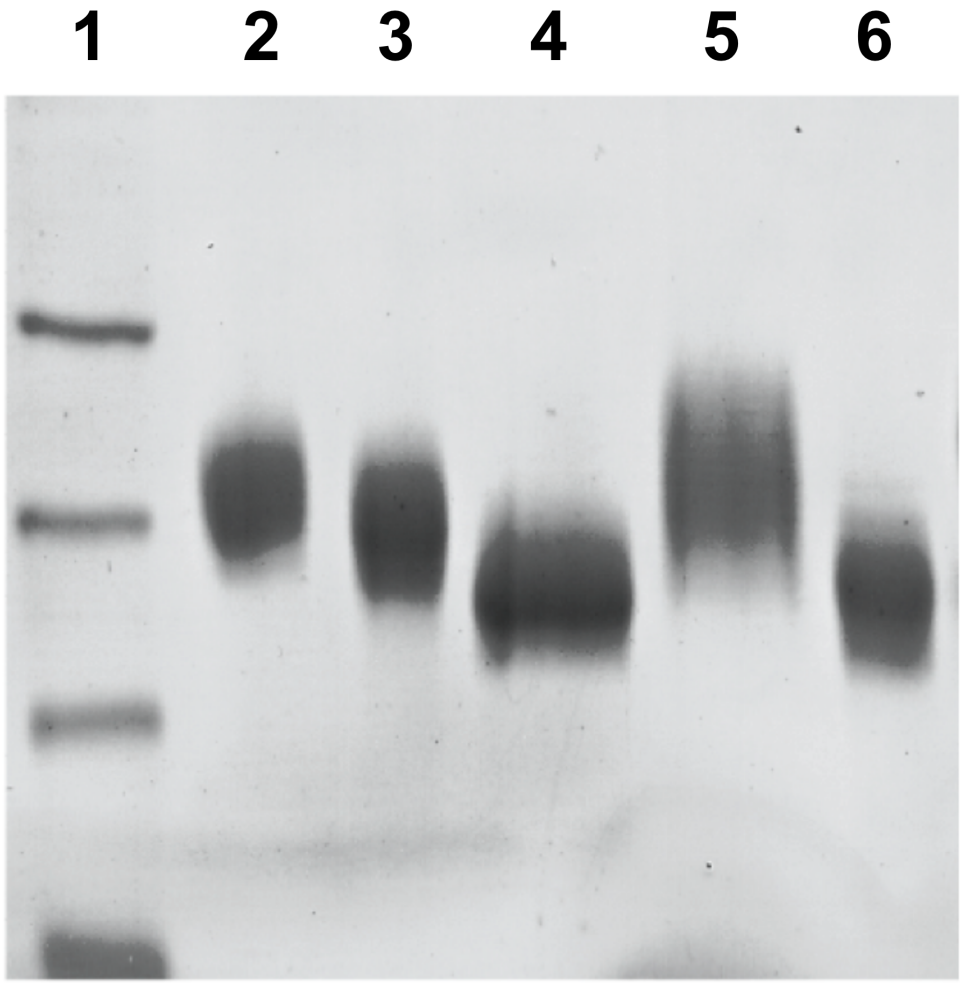

Fig. S4

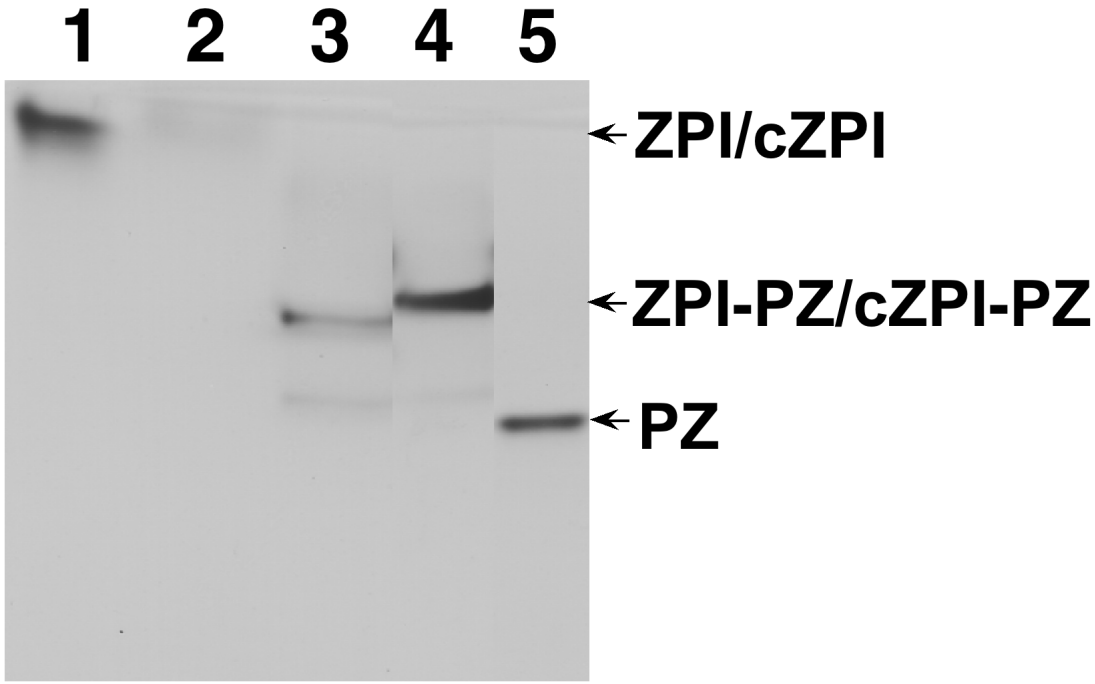

Fig. S5

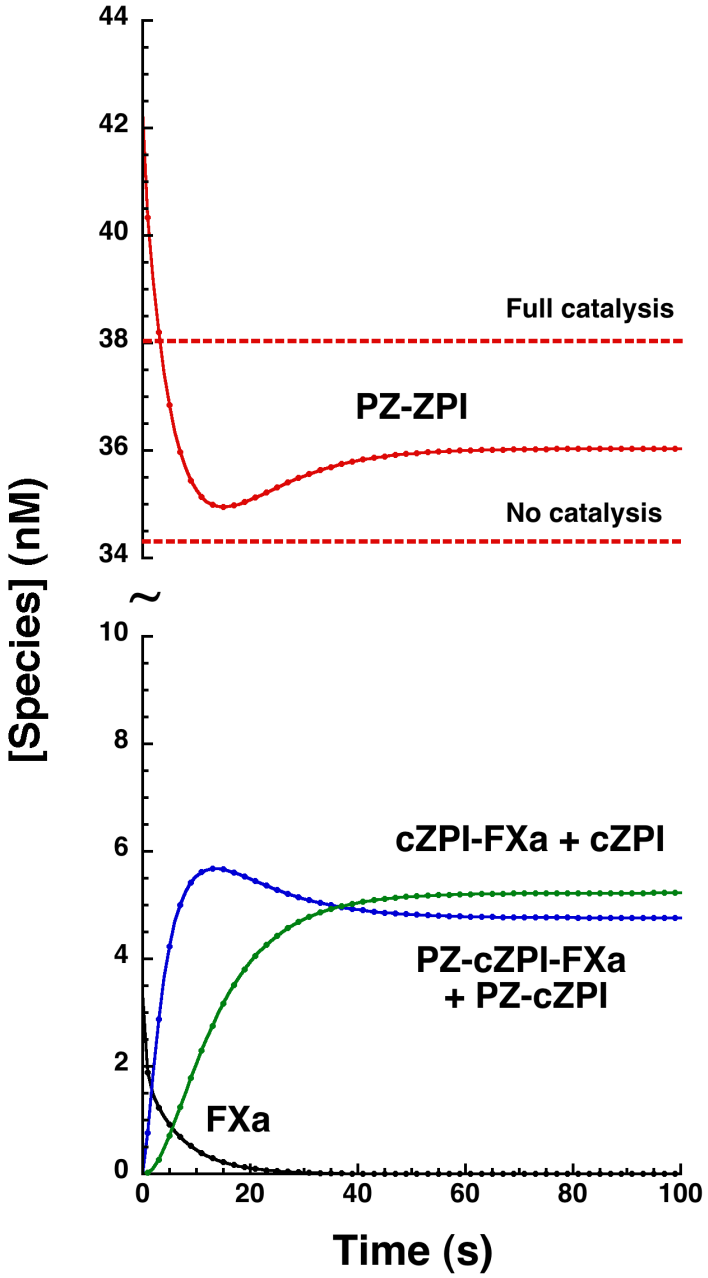
44
42
40
38
36
34
Full catalysis
PZ-ZPI
No catalysis
10
8
6
4
2
0
cZPI-FXa + cZPI
PZ-cZPI-FXa
+ PZ-cZPI
FXa
0
20
40
60
80
100
[Species] (nM)
Time (s)

Fig. S6

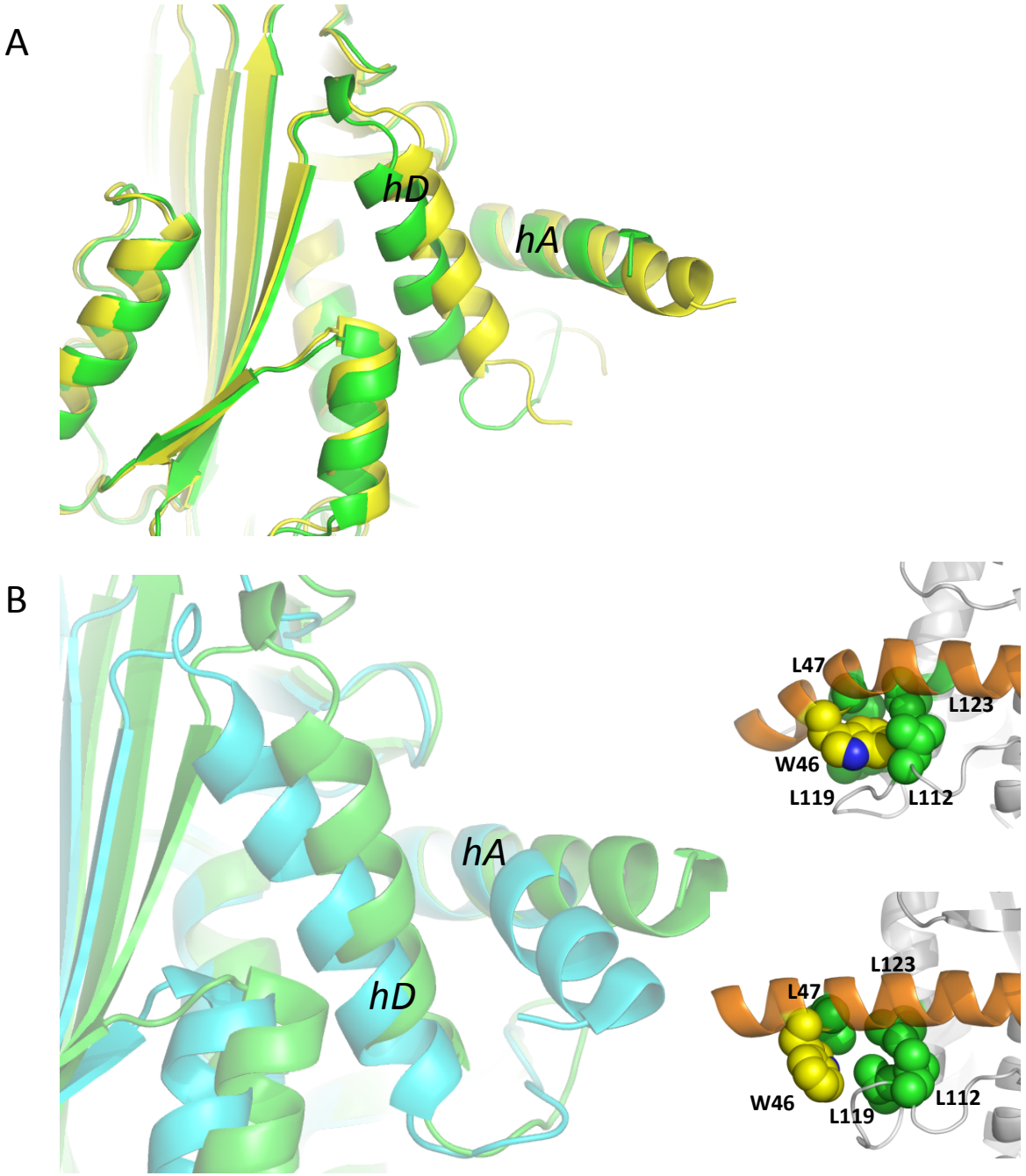

Fig. S7

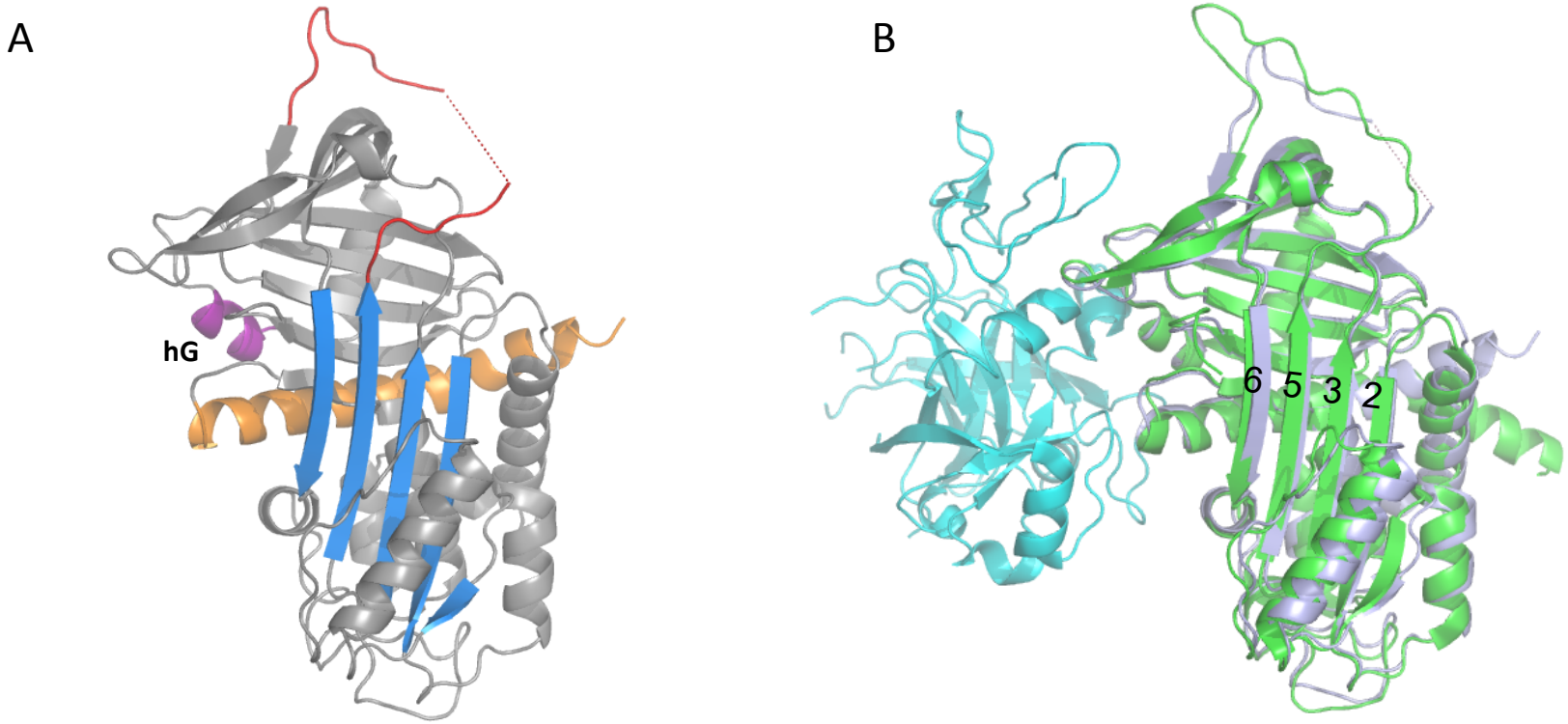

Fig. S8

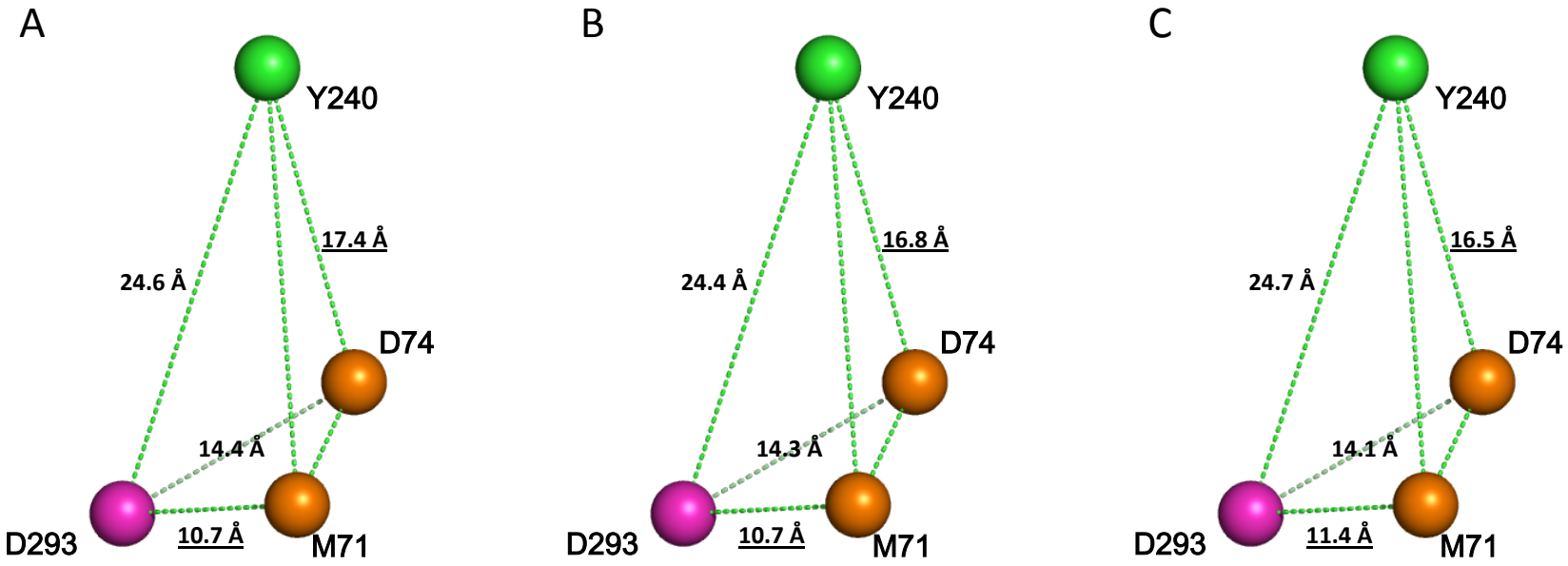

cZPI (P41) cZPI (I2) ZPI:PZ complex